MOLECULAR AND CELLULAR BIOLOGY, May 2008, p. 2896–2907 Vol. 28, No. 9
0270-7306/08/$08.00+0 doi:10.1128/MCB.01844-07

Staufen1 Regulation of Protein Synthesis-Dependent Long-Term Potentiation and Synaptic Function in Hippocampal Pyramidal Cells▽

Geneviève Lebeau,[1] Marjolaine Maher-Laporte,[2] Lisa Topolnik,[1]† Charles E. Laurent,[1] Wayne Sossin,[3] Luc DesGroseillers,[2] and Jean-Claude Lacaille[1]*

Départements de physiologie[1] et biochimie,[2] GRSNC, Université de Montréal, C.P. 6128, Succ. Centre-ville, Montréal, Québec, Canada H3C 3J7, and Department of Neurology and Neurosurgery, McGill University, Montreal, Quebec, Canada H3G 1Y6[3]

Received 10 October 2007/Returned for modification 13 November 2007/Accepted 21 February 2008

Staufen1 (Stau1) is an RNA-binding protein involved in transport, localization, decay, and translational control of mRNA. In neurons, it is present in cell bodies and also in RNA granules which are transported along dendrites. Dendritic mRNA localization might be involved in long-term synaptic plasticity and memory. To determine the role of Stau1 in synaptic function, we examined the effects of Stau1 down-regulation in hippocampal slice cultures using small interfering RNA (siRNA). Biolistic transfection of Stau1 siRNA resulted in selective down-regulation of Stau1 in slice cultures. Consistent with a role of Stau1 in transporting mRNAs required for synaptic plasticity, Stau1 down-regulation impaired the late form of chemically induced long-term potentiation (L-LTP) without affecting early-LTP, mGluR1/5-mediated long-term depression, or basal evoked synaptic transmission. Stau1 down-regulation decreased the amplitude and frequency of miniature excitatory postsynaptic currents, suggesting a role in maintaining efficacy at hippocampal synapses. At the cellular level, Stau1 down-regulation shifted spine shape from regular to elongated spines, without changes in spine density. The change in spine shape could be rescued by an RNA interference-resistant Stau1 isoform. Therefore, Stau1 is important for processing and/or transporting in dendrites mRNAs that are critical in regulation of synaptic strength and maintenance of functional connectivity changes underlying hippocampus-dependent learning and memory.

Staufen is a double-stranded RNA-binding protein that was first characterized in *Drosophila melanogaster*, where it is involved in transport and localization of *bicoid* and *oskar* mRNAs in oocytes and contributes to localization of *prospero* mRNA during neuroblast development (6, 37, 52). In mammals, two different homologues (Staufen 1 [Stau1] and Stau2) have been identified (7, 10). Stau1 is ubiquitously expressed in mammals (12, 36, 61). Whereas Stau2 is found in several tissues, it is nevertheless mainly expressed in the brain (12, 36, 61). In neurites, the two paralogues of Staufen are found in distinct RNA granules, suggesting unique functions for each protein (12, 57). A role for Staufen proteins in mRNA transport and translational control has been proposed since they are present in RNA granules that migrate within the dendrites of hippocampal neurons in a microtubule-dependent way (28, 31, 33) and regulate transport of mRNA (25, 55). Staufen proteins also associated with polysomes (12, 34, 36, 61), and Stau1 was shown to be involved in the translational control of mRNAs (13). Recently, Stau1 was shown to be involved in a specific mRNA decay pathway (30), suggesting an additional role in posttranscriptional gene control.

Localization of mRNA in neuronal dendrites has been proposed as a mechanism for establishing synaptic memory and maintaining synaptic plasticity (27, 54). There is considerable evidence for local translation in neuronal dendrites (45, 56, 58), and local translation is required for various forms of synaptic plasticity, including the late phase of transcription-dependent long-term potentiation (L-LTP), beta-adrenergic-dependent LTP, and mGluR-induced long-term depression (LTD) (5, 17, 22). Local synthesis is also important for the growth and maturation of dendritic spines (2, 43, 56, 58). Interestingly, it was also shown that down-regulation of Stau1 by small interfering RNA (siRNA) reduces CaMKII mRNA transport in cultured hippocampal neurons (25). However, the physiological consequences of Stau1 knockdown have not been examined.

In the present study we use an RNA interference technique (siRNA) combined with electrophysiological recordings in slice cultures to examine the role of Stau1 in synaptic plasticity. We find an important role for Stau1 specifically in L-LTP. Moreover, knockdown of Stau1 also revealed deficits in spine morphology and spontaneous miniature synaptic activity.

MATERIALS AND METHODS

Organotypic hippocampal slice cultures. All experiments were done in accordance with animal care guidelines at the Université de Montréal. Organotypic hippocampal slices were prepared and maintained in culture as previously described (53). In brief, Sprague-Dawley rats (postnatal day 7) were anesthetized and decapitated. The brain was removed and dissected in Hanks' balanced salt solution (Invitrogen Canada, Ontario, Canada)-based medium. Corticohippocampal slices (400 μm thick) were obtained with a McIlwain tissue chopper (Campden Instruments, IN). Slices were placed on Millicell culture plate inserts (Millipore, MA) and incubated for 3 days in OptiMem (Invitrogen Canada, Ontario, Canada)-based medium at 37°C in a humidified atmosphere of 5% CO_2 and 95% air. Inserts were then transferred to Neurobasal-based medium (In-

* Corresponding author. Mailing address: Département de physiologie, Université de Montréal, C.P. 6128 Succ. Centre-ville, Montréal, Québec, Canada H3C 3J7. Phone: (514) 343-5794. Fax: (514) 343-2111. E-mail: jean-claude.lacaille@umontreal.ca.

† Present address: Départements de biochimie et microbiologie, Division de Neurobiologie Cellulaire, Centre de Recherche Université Laval Robert-Giffard, Québec G1J 2G3, Canada.

▽ Published ahead of print on 3 March 2008.

vitrogen Canada, Ontario, Canada). Slices were used for experiments after 4 to 7 days in culture.

HEK293 cells. HEK293 cells were grown in Dulbecco's modified Eagle's medium (Invitrogen Life Science) supplemented with 10% Cosmic calf serum (HyClone, Logan, UT), 5 μg/ml penicillin-streptomycin, and 2 mM L-glutamine (Invitrogen Life Science) and maintained at 37°C saturated with 5% CO_2.

siRNAs and transfections. Enhanced cyan fluorescent protein (ECFP) (Clontech Laboratories, CA) was cloned into the pCDNA-RSV vector. pEYFP-C1 (enhanced yellow fluorescent protein [EYFP]) was obtained from Clontech Laboratories (CA). All siRNAs were purchased from Dharmacon (CO). Commercial siCONTROL was used as nontargeting control siRNA. siRNA-STAU1 target sequences for rat were 5′-GGACAGCAGUUUAAUGGGAUU-3′ (sense sequence) and 5′-PUCCCAUUAAACUGCUGUCCUU-3′ (antisense sequence). shRNA-STAU1/sh1 and plasmid coding for Stau1^{55}Δsh1 were described previously (13). HEK293 cells were seeded at 2×10^5 cells per well in a six-well plate and transfected with 60 pmol of either siRNA-CTL or siRNA-STAU1 using Lipofectamine 2000 (Invitrogen Life Science). At 24 h posttransfection, cells were transfected again with 100 pmol of the respective siRNA and 1 μg each of plasmids coding for Stau1-hemagglutinin (HA) or Stau2-HA and hnRNPH1-myc, used as control. Cells were processed for Western blotting 24 h posttransfection. Biolistic transfection of neurons in organotypic slice cultures was performed as previously described (4), using a Helios gene gun (Bio-Rad, CA) following the manufacturer's instructions. Biolistic transfection of cyanine 3-tagged nontargeting siRNA (Cy3-siRNA-CTL) and confocal microscopy following fixation of slice cultures were used to verify siRNA delivery in pyramidal cells. Electrophysiological recordings and cell imaging experiments were performed 48 h after transfection, and the experimenter was blind to transfection treatments.

Electrophysiology. Individual slice cultures were transferred to a submerged recording chamber and continuously perfused (at 1 to 2 ml/min) with artificial cerebrospinal fluid composed of 124 mM NaCl, 2.5 mM KCl, 1.25 mM NaH_2PO_4, 1.3 mM $MgSO_4$, 26 mM $NaHCO_3$, 10 mM dextrose, and 2.5 mM $CaCl_2$ (5 mM KCl, 2 mM $MgSO_4$, and 2 mM $CaCl_2$ for LTD experiments), saturated with 95% O_2 and 5% CO_2, pH 7.4. Extracellular field excitatory postsynaptic potentials (fEPSPs) were recorded from CA1 stratum radiatum with a glass microelectrode (2 to 3 MΩ) filled with 2 M NaCl in slices maintained at 25 to 27°C. A bipolar tungsten electrode placed in stratum radiatum was used for electrical stimulation of Schaffer collaterals. Stimulus intensity (0.1-ms duration) was adjusted to elicit 30 to 40% of the maximal fEPSP, as determined by an input-output curve for each slice (LTD, 60% of maximal value). To reduce spontaneous activity, CA1 and CA3 hippocampal regions were isolated by a surgical cut. L-LTP was induced chemically by the adenylate cyclase activator forskolin (FSK; 50 μM; Sigma) (26, 32). The early phase of LTP (E-LTP) was induced using either high-frequency stimulation (HFS; 100 pulses at 100 Hz applied twice with a 5-min interval) or theta burst stimulation (TBS; four pulses at 100 Hz per burst, five bursts at 5 Hz per train) applied twice at 10-s intervals. LTD was induced chemically by the group I metabotropic glutamate receptor (mGluR) agonist (*S*)-3,5-dihydroxyphenylglycine (DHPG; 100 μM; Tocris). Miniature excitatory postsynaptic currents (mEPSCs) were recorded in whole-cell patch-clamp mode from EYFP-transfected CA1 pyramidal cells using an Axopatch 200B amplifier (Axon Instruments, Foster City, CA) in slices maintained at 27 to 32°C. Recording pipettes (4 to 5 MΩ) were filled with a solution containing 130 mM $CsMeSO_3$, 5 mM CsCl, 2 mM $MgCl_2$, 5 mM diNa-phosphocreatine, 10 mM HEPES, 2 mM ATP-Tris, and 0.4 mM GTP-Tris, pH 7.2 to 7.3, 275 to 285 mOsm. Bicuculline (10 μM) and tetrodotoxin (0.5 μM) were added to the extracellular solution, and cells were voltage clamped at −60 mV. Data acquisition (filtered at 2 kHz, digitized at 10 kHz) and analysis were performed using a personal computer equipped with pClamp9 software (Molecular Devices). Threshold mEPSC amplitude was set at 3 pA, and typically 150 to 250 events were collected over a 10- to 20-min period.

Immunocytochemistry. Rat primary hippocampal neurons were dissected from embryonic day 17 to 19 Sprague-Dawley embryos (Charles River Laboratories) and cultured as described previously (3, 14). Briefly, neurons were plated at 80,000 cells/ml on 18-mm-diameter glass coverslips (Fisher Scientific) coated with 0.1% poly-D-lysine. Transfections of 20 pmol of siRNA and 0.3 μg of plasmid coding for ECFP were performed with 2 μl of Lipofectamine 2000 reagent (Invitrogen). At 48 h posttransfection, neurons were fixed with 4% paraformaldehyde-4% sucrose in phosphate-buffered saline (PBS) for 20 min. Neurons were then permeabilized with 0.3% Triton X-100–2% bovine serum albumin in PBS for 10 min, blocked with 0.1% Triton X-100–2% bovine serum albumin in PBS for 45 min, and further washed with the same solution. Neurons were incubated with 2 μg/ml mouse anti-CFP (Roche) and rabbit anti-Stau1 (1:100) (61) antibodies for 1 h, washed, and stained with Alexa Fluor 488 dye–anti-mouse immunoglobulin G (IgG) or Alexa Fluor 594 dye–anti-rabbit IgG antibodies (Molecular Probes) for 1 h. Following the immunolabeling procedure, some neuron cultures (as indicated) were incubated with 10 μM of Syto14 (Invitrogen S7576) for 15 min. Coverslips were mounted on slides (Fisher) using Dako fluorescent mounting medium (Dako). Neurons were visualized under an Olympus fv300 confocal microscope using a UPLFL 60× 1.40-numerical-aperture oil-immersion objective lens. Hippocampal slices were fixed in 4% paraformaldehyde in 0.1 M phosphate buffer (4°C, overnight). Slices were cryoprotected in 30% sucrose and recut (60 μm thick) on a freezing microtome (Leica SM2000R; Germany). Sections were treated with 0.3% H_2O_2 (30 min), preincubated with 2% normal goat serum and 0.2% Triton X-100 in 0.1 M PBS for 2 h at room temperature (RT), and then incubated with primary mouse monoclonal NeuN antibody (1:250; overnight at RT; Chemicon, CA). The next day, sections were placed in biotinylated secondary goat anti-mouse IgG antibody (1:500; 2 h at RT; Vector Laboratories). Sections were then reincubated in the avidin-biotin complex (Elite ABC kit; Vector Laboratories; 1:200; 2 h) and visualized using 3,3′-diaminobenzidine. Sections were rinsed thoroughly between incubations and mounted in DPX mounting medium.

Western blotting. Protein samples from hippocampal slice or human embryonic kidney cell extract were separated on a 10% sodium dodecyl sulfate-polyacrylamide gel and transferred onto an Amersham Hybond-P (polyvinylidene difluoride) membrane. Immunoblot assays were performed in PBS-0.2% Tween 20 with specific antibodies.

Imaging and morphological analysis. Slices were fixed with 4% paraformaldehyde overnight at 4°C, washed in phosphate buffer, and mounted on slides for confocal microscopy. EYFP-transfected CA1 pyramidal neurons were randomly selected based on green fluorescence and characteristic morphology. For spine analysis, Z-stacks consisting of 10 to 20 sections (512 × 512 pixels, 30- to 100-μm-long dendritic segments) spaced 0.2 to 0.4 μm apart were collected from the secondary branches of apical dendrites using a confocal laser scanning microscope (LSM 510; Carl Zeiss, Kirkland, Quebec, Canada) equipped with a 63× oil-immersion objective (numerical aperture, 1.4; Carl Zeiss, Kirkland, Quebec, Canada). The length and morphology of dendritic spines were measured using the LSM 510 software. Four to six independent experiments were performed, and 1,784 protrusions were analyzed from 72 neurons.

Statistical analysis. Baseline synaptic transmission was monitored for 15 min or 30 min (LTP experiments) and 20 min (LTD experiments) before the induction stimulation protocol or drug administration. The slope of fEPSPs was expressed as a percentage of the baseline average before induction or drug application. Every data point represents an average of normalized data in bins of 2 min (E-LTP), 5 min (L-LTP), or 2.5 min (LTD). Statistical differences were compared between baseline values and values after induction or drug application (Student's paired *t* test). Data are represented as means ± standard errors of the means, unless otherwise mentioned, and statistical significance was set at $P < 0.05$. Differences between all transfected groups were assessed with analysis of variance tests. Comparisons of cumulative distribution of spine length and mEPSC parameters between groups were performed using Kolmogorov-Smirnov tests.

RESULTS

Down-regulation of Stau1 by siRNA transfection. To determine that siRNA can be used for a selective knockdown of Stau1, we tested the efficacy and specificity of the siRNA targeting Stau1 (siRNA-STAU1) by Western blot analysis in human embryonic kidney cells (HEK293), hippocampal neurons in cultures, and hippocampal slice cultures. First, HEK293 cells were cotransfected with plasmids coding for mStau1-HA and hnRNPH1-myc (used as control) and either a nontargeting siRNA (siRNA-CTL) or an siRNA directed against Stau1 (siRNA-STAU1) (Fig. 1A and B). Western blot analyses with anti-HA and anti-myc antibodies indicated a significant reduction in the amounts of Stau1-HA relative to hnRNPH1-myc (90.0% ± 3.9% reduction; $n = 3$; $P < 0.05$; Student's *t* test) when cotransfected with siRNA-STAU1, compared to siRNA-CTL (Fig. 1A). When plasmids coding for Stau2-HA instead of Stau1-HA were transfected in HEK293 cells, no decrease in the expression of the proteins was observed in the presence of siRNA-STAU1 compared to siRNA-CTL (Fig. 1B). These re-

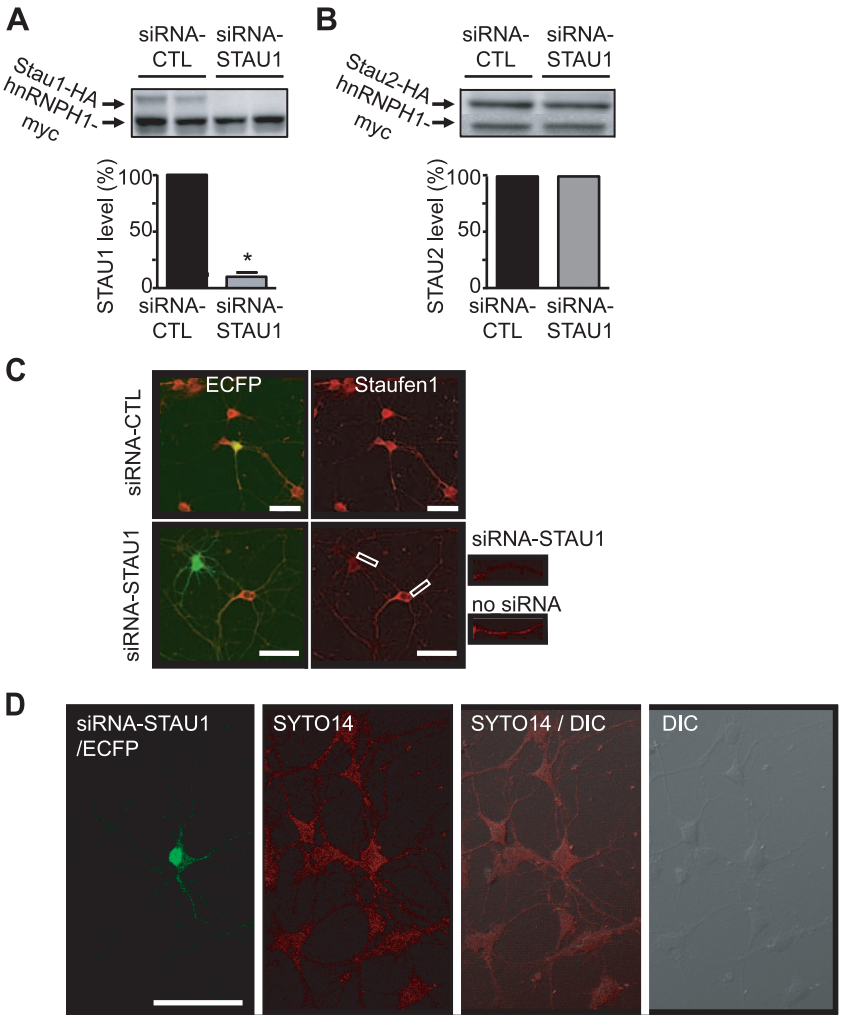

FIG. 1. Down-regulation of Stau1 by siRNA in HEK293 cells and in cultured hippocampal neurons. (A and B) HEK293 cells were cotransfected with plasmids coding for hnRNPH1-myc and either mStau1-HA (A) or mStau2-HA (B) and either siRNA-CTL or siRNA-STAU1. Expression of the proteins was monitored by Western blotting using anti-HA and anti-myc antibodies and plotted as the percentage of expression of Stau1-HA compared to that of hnRNPH1-myc. Expression of Stau1-HA in cells with siRNA-CTL was set to 100%. The protein expression level (%) of Stau1, but not of Stau2, is significantly down-regulated in cells transfected with siRNA-STAU1. (C) Immunostaining for Stau1 in untransfected neurons and in neurons coexpressing ECFP and siRNA-CTL (top) or ECFP and siRNA-STAU1 (bottom). Stau1 expression was decreased in siRNA-STAU1-transfected cells compared to untransfected cells. Bars, 50 μm. (D) Syto14 labeling in untransfected neurons and in neurons coexpressing ECFP and siRNA-STAU1. Stau1 down-regulation does not prevent the overall transport of mRNA in dendrites, suggesting that Stau1 inhibits specific mRNA targets. Bar, 50 μm.

sults indicate that transfection of siRNA-STAU1 is efficient in down-regulating the expression of Stau1 and that the down-regulation is specific, leaving Stau2 levels intact. Next, we tested the efficacy of siRNA-STAU1 transfection in down-regulating endogenous Stau1. Hippocampal neurons in cultures were transfected with either siRNA-CTL or siRNA-STAU1 along with a plasmid coding for ECFP as a marker for transfected cells. Immunofluorescence studies using anti-Stau1 antibody were then performed to evaluate Stau1 expression in individual neurons. An important decrease in Stau1 signal was observed in neurons transfected with siRNA-STAU1 compared to untransfected cells in the same culture (Fig. 1C). In contrast, no decrease was seen in neurons transfected with the siRNA-CTL (Fig. 1C). Then, we determined whether the knockdown expression of Stau1 impairs global mRNA transport in dendrites. Cultured neurons were transfected with siRNA-STAU1 along with a plasmid coding for ECFP as a marker for transfected cells. Neurons were labeled with Syto14, a dye that stains RNA, and visualized on a confocal microscope. Comparison of siRNA-STAU1-transfected cells, siRNA-CTL-transfected cells (data not shown), and surrounding untransfected cells showed no difference in the global staining of RNA in dendrites (Fig. 1D). Therefore, although knockdown expression of Stau1 was shown to impair the dendritic transport of a transcript containing the 3′ untranslated region of αCaMKII (25), it does not prevent the overall transport of mRNA in dendrites, suggesting that Stau1 inhibits specific mRNA targets.

Then, Stau1 knockdown was tested in hippocampal slice cultures that were biolistically transfected at 4 days in vitro with plasmids coding for EYFP and either siRNA-CTL or

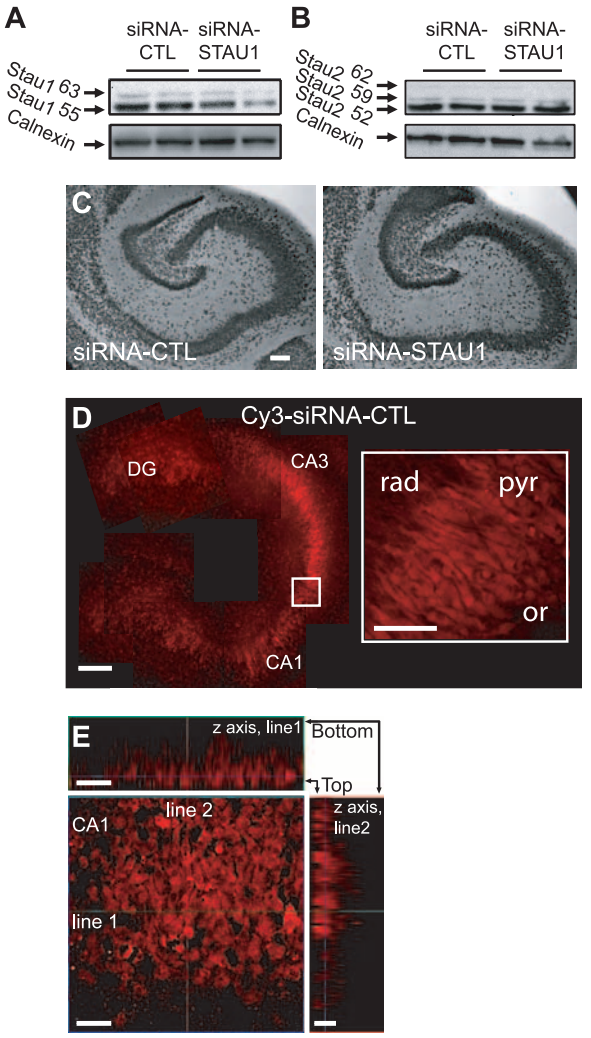

FIG. 2. Down-regulation of Stau1 by siRNA in organotypic hippocampal slice cultures. (A and B) Slice cultures were biolistically transfected with siRNA-CTL or siRNA-STAU1. Protein expression was monitored by Western blotting using anti-Stau1 (A) or anti-Stau2 (B) antibodies. Examples from four representative slices are shown, illustrating the selective down-regulation of endogenous Stau1 but not Stau2 expression levels ($n = 6$, two experiments). (C) Immunocytochemical labeling for NeuN, showing intact neuronal populations in hippocampal slice cultures biolistically transfected with siRNA-CTL or siRNA-STAU1. Bar, 100 μm. (D and E) Confocal images of representative hippocampal slice cultures biolistically transfected with Cy3-siRNA-CTL, illustrating delivery of siRNA in CA1 pyramidal cells (D) and localization in superficial tissue in slices (Z-stack projections in panel E). Inset, CA1 region; or, stratum oriens; pyr, stratum pyramidale; rad, stratum radiatum. Bars, 100 μm (D), 50 μm (inset in panel D), and 20 μm (E).

siRNA-STAU1. Two days posttransfection, slices were homogenized and proteins were analyzed by Western blotting using anti-Stau1 antibodies (Fig. 2A). Anticalnexin antibodies were used as a loading control. Transfection of siRNA-STAU1 caused a significant reduction in the expression level of endogenous Stau1 (Fig. 2A) but not of endogenous Stau2 (Fig. 2B) in slice cultures. The neuronal integrity of transfected slice cultures was verified using NeuN immunolabeling, and the transfection procedure did not lead to cell loss (Fig. 2C). The knockdown in expression of endogenous Stau1 in organotypic hippocampal slice cultures was more variable than that observed with overexpression of tagged Stau1 in HEK293 cells, ranging from 70% reduction to almost no reduction (average of 31.7% ± 10.5%; $n = 6$; two independent experiments; $P < 0.05$; Student's t test). This variability probably reflects the reduced efficiency of transfection in hippocampal slice cultures. To examine this more carefully, we measured the delivery and localization of siRNA in CA1 pyramidal cells in slices using a cyanine-3-tagged control siRNA (Cy3-siRNA-CTL) and confocal microscopy ($n = 6$ to 9; two experiments) (Fig. 2D and E). We observed that the biolistic transfection mostly occurs at superficial levels of the slice, since we found a strong signal in the majority of superficial neurons and a clear gradient of the Cy3-siRNA-CTL from the surface of the slice through deeper levels (z axis). Thus, there was only an efficient delivery/transfection in the first 20 to 50 μm of tissue in the slices, presumably resulting in specific knockdown of STAU1 only in more superficial neurons, which fortuitously are the same as those recorded in electrophysiology experiments (see below). Since the entire slices were taken for Western blot experiments, the results from this analysis underestimate the knockdown in the neurons recorded in field recording experiments. Taken together, these experiments demonstrate the efficacy and specificity of Stau1 siRNA transfection in down-regulating Stau1 expression in cultured slices.

Stau1 down-regulation impairs specifically L-LTP. Local translation of mRNAs in dendrites is known to play an important role in synaptic plasticity (27, 51). Stau1 is a putative candidate protein that may be involved in the regulation of synaptic plasticity, since it has been implicated in mRNA trafficking to neuronal dendrites (25, 29) and in translational regulation (13). Therefore, we examined the effect of Stau1 down-regulation on long-lasting changes in synaptic plasticity that require transcription and translation (26, 32, 41). Since standard electrical stimulation protocol (four tetanic trains) for inducing the late form of LTP in acute slices does not reliably induce L-LTP in slice cultures (32) and since we wished to maximize the number of synapses that undergo plasticity, LTP was induced chemically, using FSK (32, 44). FSK elevates cyclic AMP concentrations by activating adenylate cyclase (8, 21, 62) and elicits spontaneous activity in slice cultures that induce *N*-methyl-D-aspartic acid (NMDA) receptor-dependent L-LTP (32, 44). Hippocampal slices were biolistically transfected with plasmid coding for EYFP or cotransfected with EYFP plasmid and either siRNA-CTL or siRNA-STAU1. fEPSPs were recorded in area CA1 of the hippocampus. In control conditions, application of FSK induced a potentiation of fEPSPs lasting at least 3.5 h (142% ± 14.5% of control for EYFP and 136% ± 8.8% of control for siRNA-CTL transfections; $n = 10$ each; $P < 0.05$) (Fig. 3A to E). In slices cotransfected with plasmid encoding EYFP and siRNA-STAU1, FSK-induced LTP was blocked (106.7% ± 10.8% of control at 210 min post-FSK application; $n = 10$; $P > 0.05$) (Fig. 3A to E). FSK induced similar spontaneous activities in all three conditions, indicating that the block of L-LTP was not due to a failure of FSK to elicit spontaneous activity necessary for LTP induction. To confirm the type of L-LTP induced in our slice culture conditions, we carried out additional control experiments with the NMDA receptor antagonist D,L-2-amino-5-

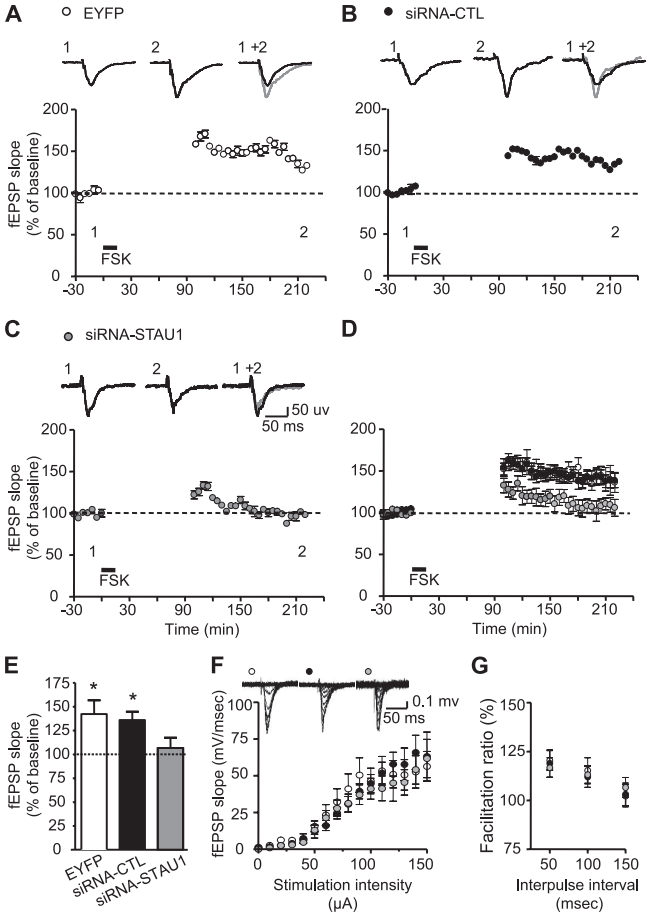

FIG. 3. Stau1 siRNA transfection impairs chemically induced L-LTP in hippocampal slice cultures. (A to C) Plots of normalized fEPSP slope in representative experiments with slice cultures transfected with plasmids coding for EYFP alone (A) or in combination with siRNA-CTL (B) or siRNA-STAU1 (C). Corresponding field potentials before (black line) and after (gray line) FSK application (50 μM, 15 min) are shown above. fEPSP measures for the period from 0 to 90 min were excluded because of FSK-induced spontaneous activity interfering with accurate measurements of evoked fEPSPs (32). (D) Summary plots of fEPSP changes for all group data ($n = 10$ slices in each condition). (E) Summary bar graph showing changes in fEPSP slope at 220 min post-FSK application. Significant L-LTP was present in slices transfected with EYFP and siRNA-CTL but absent in slices transfected with siRNA-STAU1, indicating that down-regulation of Stau1 prevents L-LTP. *, $P < 0.05$. (F) Graph of input-output relation of fEPSP slope as a function of stimulation intensity, indicating no significant difference between groups with EYFP (white dots), siRNA-CTL (black dots), or siRNA-STAU1 (gray dots) transfection. (G) Summary plot for all slices showing similar paired-pulse facilitation ratio (50- to 150-ms intervals) in groups with EYFP (white dots), siRNA-CTL (black dots), or siRNA-STAU1 (gray dots) transfection.

phosphonovaleric acid (AP5) and the transcription inhibitor actinomycin D. The FSK-induced L-LTP was blocked by actinomycin D and AP5 (vehicle, 151.35% ± 11% of control at 180 min post-FSK application, $n = 5$, $P < 0.05$; actinomycin D, 107.17% ± 17.7%, $n = 6$, $P > 0.05$; AP5, 110% ± 21%, $n = 6$, $P > 0.05$). Thus, these results complement those obtained in other studies (32, 44) and show that FSK-induced L-LTP is NMDA receptor and protein synthesis dependent and displays key features of standard electrically induced L-LTP. To verify that basal evoked synaptic transmission was unaffected by Stau1 down-regulation, we examined the input-output relation and paired-pulse facilitation ratio (at intervals of 50 to 150 ms) of fEPSPs. No significant differences were found between slices transfected with plasmid encoding EYFP, siRNA-CTL, or siRNA-STAU1 for input-output function ($n = 8$ to 12; $P > 0.05$) (Fig. 3F) or paired-pulse facilitation ($n = 10$ to 14; $P > 0.05$) (Fig. 3G). These results indicate that Stau1 down-regulation by siRNA prevented L-LTP but did not affect basal evoked synaptic transmission.

We next tested whether Stau1 down-regulation also affects the early phase of LTP (E-LTP). Two protocols were used to induce E-LTP, TBS and HFS. TBS generated similar E-LTP of fEPSP slope in slices transfected with EYFP (131.9% ± 5.6% of control), siRNA-CTL (134.9% ± 8.2% of control), or siRNA-STAU1 (140.7% ± 9.7% of control; $n = 6$ to 8; $P > 0.05$) (Fig. 4A to D). Similar E-LTP results were obtained following HFS of slices transfected with EYFP expressor (133.6% ± 9.7% of control), siRNA-CTL (135.1% ± 13.1% of control), or siRNA-STAU1 (136.4% ± 17.1% of control; $n = 4$ to 5; $P > 0.05$) (Fig. 4F and G). Thus, transfection of siRNA-STAU1 did not impair E-LTP, indicating that Stau1 down-regulation interferes specifically with the induction or expression of L-LTP.

Next, we determined whether LTD is affected by Stau1 down-regulation. Transient activation of mGluR1/5 by application of the selective agonist DHPG produces an LTD of excitatory synaptic responses in CA1 pyramidal cells which requires local translation of dendritic mRNAs in mature neurons but is translation independent earlier in development, such as in the present experiments (15, 22, 23, 60). As expected, application of DHPG (100 μM, 10 min) induced LTD of fEPSPs in control slice cultures transfected with plasmid coding for EYFP (62.2% ± 7% of control) or cotransfected with siRNA-CTL (66.7% ± 7.7% of control; $n = 10$) (Fig. 5A and B). Transfection of slice cultures with siRNA-STAU1 did not affect DHPG-induced LTD either (61.3% ± 2.8% of control, $n = 10$; $P > 0.05$) (Fig. 5C to E), indicating that Stau1 down-regulation does not impair translation-independent mGluR-mediated LTD in the CA1 hippocampal area.

Stau1 down-regulation reduces miniature synaptic activity. We next tested whether the deficit in L-LTP after Stau1 down-regulation was associated with functional changes at unitary excitatory synapses. We recorded mEPSCs in EYFP-transfected CA1 pyramidal cells voltage clamped at −60 mV and examined the effect of siRNA on amplitude and frequency of synaptic activity (Fig. 6A). Given that short hairpin RNA (shRNA) transfection can trigger off-target effects which affect passive membrane properties, including membrane capacitance and input resistance (1), we first determined whether siRNA transfection in our experiments might produce similar off-target actions. The membrane capacitance (c_m) and input resistance (R_{in}) of transfected pyramidal cells were comparable between the three conditions (EYFP, $R_{in} = 193.8 \pm 33.6$ MΩ and $c_m = 18.5 \pm 2.4$ pF; siRNA-CTL, $R_{in} = 185 \pm 22.8$ MΩ and $c_m = 18.6 \pm 1.3$ pF; siRNA-STAU1, $R_{in} = 196.1 \pm 14.3$ MΩ and $c_m = 22.6 \pm 2.2$ pF; $n = 7$, $P > 0.05$). The lack of impairment in passive membrane properties after siRNA transfection suggests no such off-target effects of the siRNAs used (1). In contrast, Stau1 siRNA transfection affected min-

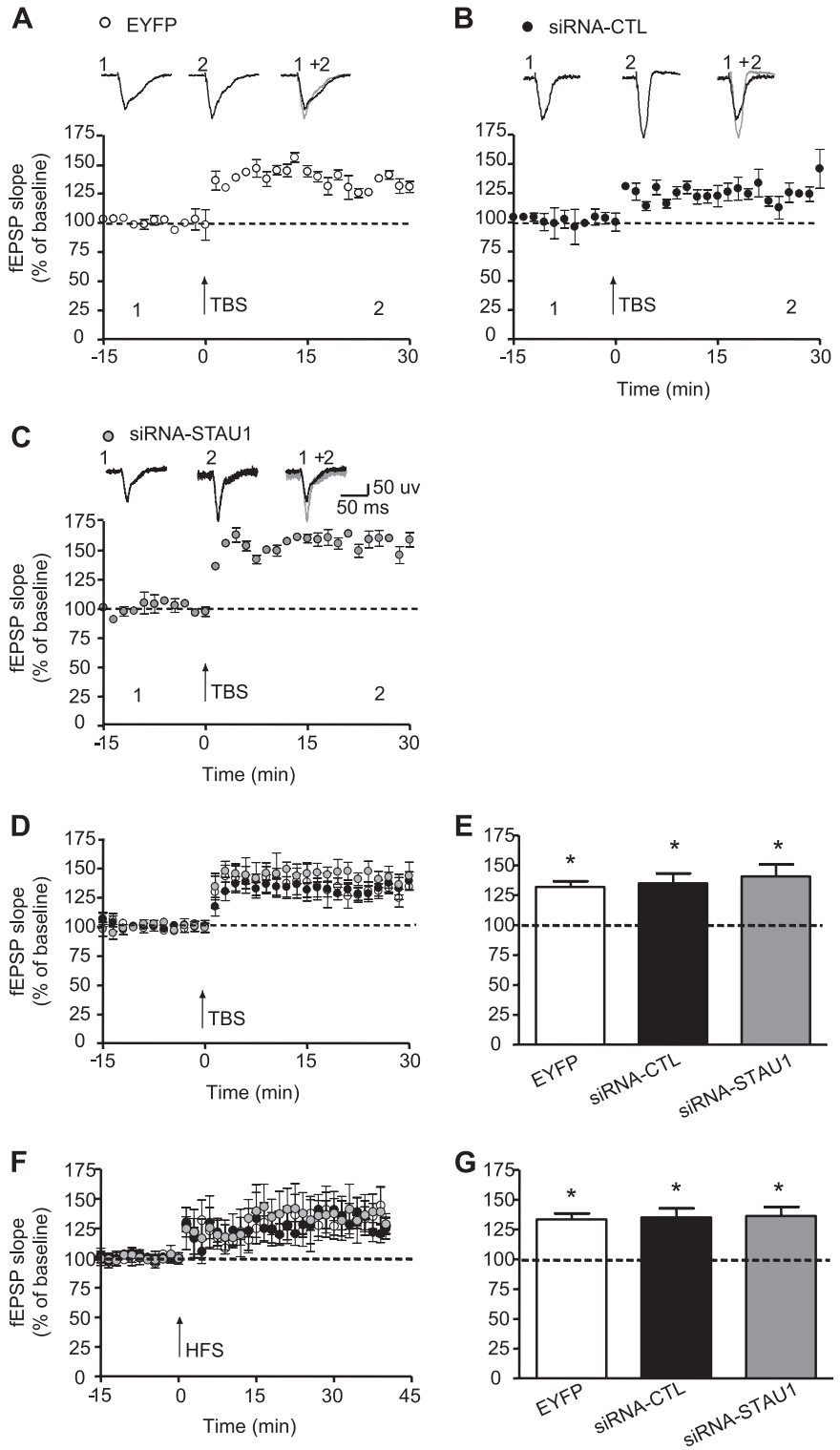

FIG. 4. Stau1 siRNA transfection does not impair E-LTP in hippocampal slice cultures. (A to C) Plots of normalized fEPSP slope showing E-LTP induced by TBS (arrow) in slice cultures transfected with plasmids coding for EYFP alone (A) or in combination with siRNA-CTL (B) or siRNA-STAU1 (C). Corresponding field potentials before (black line) and after (gray line) TBS are shown above. (D) Summary plots of fEPSP changes induced by TBS for all groups ($n = 6$ slices in each condition). (E) Summary bar graph showing LTP of fEPSP slope at 30 min post-TBS in all conditions and indicating that Stau1 siRNA transfection did not impair TBS-induced E-LTP. (F and G) Similar summary plots (F) and bar graph (G) of fEPSP changes induced by HFS (arrow) for all groups ($n = 4$ to 5 slices in each condition), illustrating that Stau1 did not influence HFS-induced E-LTP. *, $P < 0.05$ (E and G). Dots in panels E and F are as defined for panels A to C.

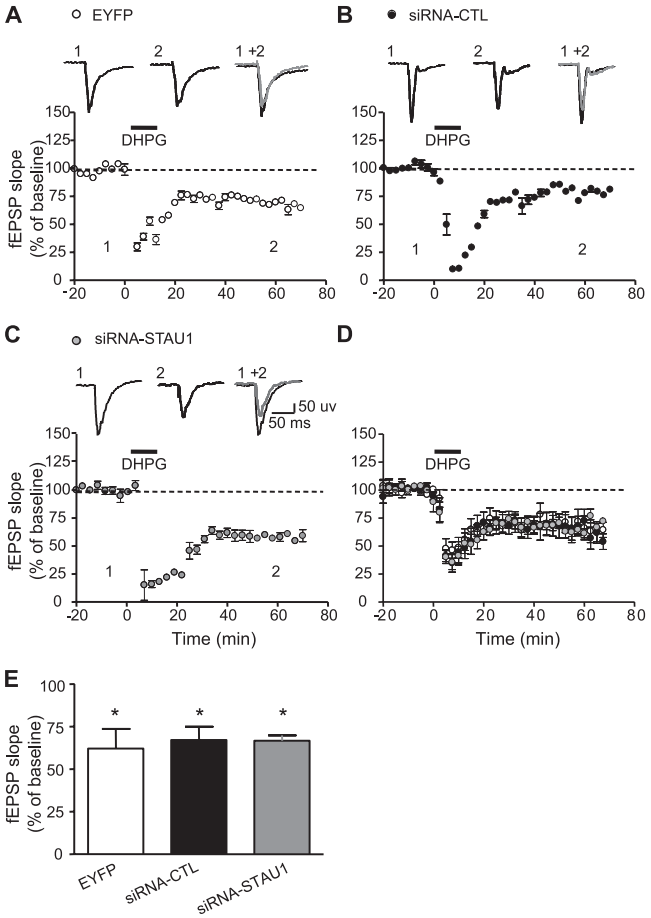

FIG. 5. Stau1 siRNA transfection does not affect mGluR-dependent LTD in hippocampal slice cultures. (A to C) Plots of normalized fEPSP slope showing LTD induced by the mGluR1/5 agonist DHPG (100 μM, 10 min) in slice cultures transfected with plasmids coding for EYFP alone (A) or in combination with siRNA-CTL (B) or siRNA-STAU1 (C). Corresponding field potentials before (black line) and after (gray line) DHPG application are shown above. (D) Summary plots of fEPSP changes induced by DHPG for all groups ($n = 10$ slices in each condition). Dots in panel D are as defined for panels A to C. (E) Summary bar graph showing LTD of fEPSP slope at 80 min post-DHPG application in all conditions and indicating that Stau1 siRNA transfection did not impair mGluR-dependent LTD. *, $P < 0.05$.

iature synaptic activity. The cumulative distribution of mEPSC amplitude was significantly decreased in neurons transfected with siRNA-STAU1 relative to neurons transfected with EYFP or siRNA-CTL ($n = 7$ each, three to five slices, 10 independent experiments; $P < 0.05$, Kolmogorov-Smirnov test) (Fig. 6B). The median of cumulative histograms for mEPSC amplitudes in neurons transfected with siRNA-STAU1 was significantly different from that in neurons transfected with EYFP or siRNA-CTL (median ± standard deviation; EYFP, −18.5 ± 10.9 pA; siRNA-CTL, −20.5 ± 10.9 pA; siRNA-STAU1, −11.75 ± 7 pA; $P < 0.001$) (Fig. 6B). Also, the cumulative distribution of inter-mEPSC interval was significantly increased in neurons transfected with siRNA-STAU1 ($P < 0.05$, Kolmogorov-Smirnov test) (Fig. 6C). In this case, the median of cumulative histograms for mEPSC inter-event interval in neurons transfected with siRNA-STAU1 was significantly different from that in neurons transfected with EYFP or siRNA-CTL (EYFP, 0.83 ± 0.8 s; siRNA-CTL, 0.8 ± 0.7 s; siRNA-STAU1, 1.54 ± 1.3 s; $P < 0.001$) (Fig. 6C). Decreases in mEPSC amplitude are most consistent with postsynaptic modifications of synapses (receptor numbers or sensitivity), whereas decreases in mEPSC frequency are associated with changes in presynaptic transmitter release or in number of functional synapses (35, 47). Thus, the observed effects on miniature synaptic activity suggest that Stau1 down-regulation is associated with both a reduction of postsynaptic efficacy at individual synapses and a decrease in number of functional synapses or changes in presynaptic transmitter release in pyramidal cells.

Stau1 down-regulation induces dendritic spine morphology changes. In hippocampal pyramidal neurons, dendritic spines act as independent cellular compartments enabling selective regulation of individual synapses (20, 63). Moreover, the morphology and density of dendritic spines reflect the properties and number of synapses (20, 63). For instance, elongated spines are associated with smaller postsynaptic densities (PSDs) and a higher proportion of silent synapses (20, 38, 42). Therefore, we next examined if changes in unitary synaptic function after Stau1 down-regulation were associated with changes of spine density and morphology in hippocampal CA1 pyramidal cells. Hippocampal slices were transfected with plasmids coding for EYFP or cotransfected with siRNA-CTL or siRNA-STAU1. First, confocal imaging of EYFP-labeled cells indicated no obvious alteration in the general dendritic arborization of transfected cells in any groups (Fig. 7A). Second, the overall spine density was not significantly different among cells transfected with EYFP alone (0.24 ± 0.01 spines/μm), siRNA-CTL plus EYFP (0.25 ± 0.02 spines/μm), or siRNA-STAU1 plus EYFP (0.26 ± 0.02 spines/μm; $P > 0.05$) (Fig. 7B), indicating no significant loss of spines in cells of any group. However, significant differences were observed at the level of spine morphology. The length of dendritic spines was significantly longer in cells cotransfected with siRNA-STAU1 plus EYFP than in cells transfected with EYFP alone (128.76% ± 4.38% of control EYFP) or cotransfected with siRNA-CTL plus EYFP (125.65% ± 4.27% of control siRNA-CTL; $P < 0.05$; $n =$ 472, 474, and 486 protrusions in EYFP, siRNA-CTL plus EYFP, and siRNA-STAU1 plus EYFP groups, respectively; $n = 4$ to 6 separate experiments) (Fig. 7C). The cumulative distribution of spine lengths was significantly different in cells cotransfected with siRNA-STAU1 plus EYFP than in cells transfected with EYFP alone (Fig. 7C) ($P < 0.05$).

To characterize further the changes in spine morphology, we examined changes in different classes of spines categorized on the basis of spine length and shape (39): 1, filopodia, long protrusions (>1 μm) without a spine head; 2, elongated spines, long protrusions (>1 μm) with a small head at the tip; and 3, regular spines, short protrusions (<1 μm) including stubby and mushroom-type spines. Our data showed that in cells cotransfected with siRNA-STAU1 plus EYFP, there was a significant increase in the proportion of elongated spines (137.61% ± 4.58% compared to EYFP alone [EYFP]; 127.80% ± 4.38% compared to siRNA-CTL plus EYFP [siRNA-CTL]; $P < 0.05$) (Fig. 7D) and filopodia (206.11% ± 4.67% compared to EYFP alone [EYFP]; 185.03% ± 4.65% compared to siRNA-CTL plus EYFP [siRNA-CTL]; $P < 0.05$) (Fig. 7D) and a significant

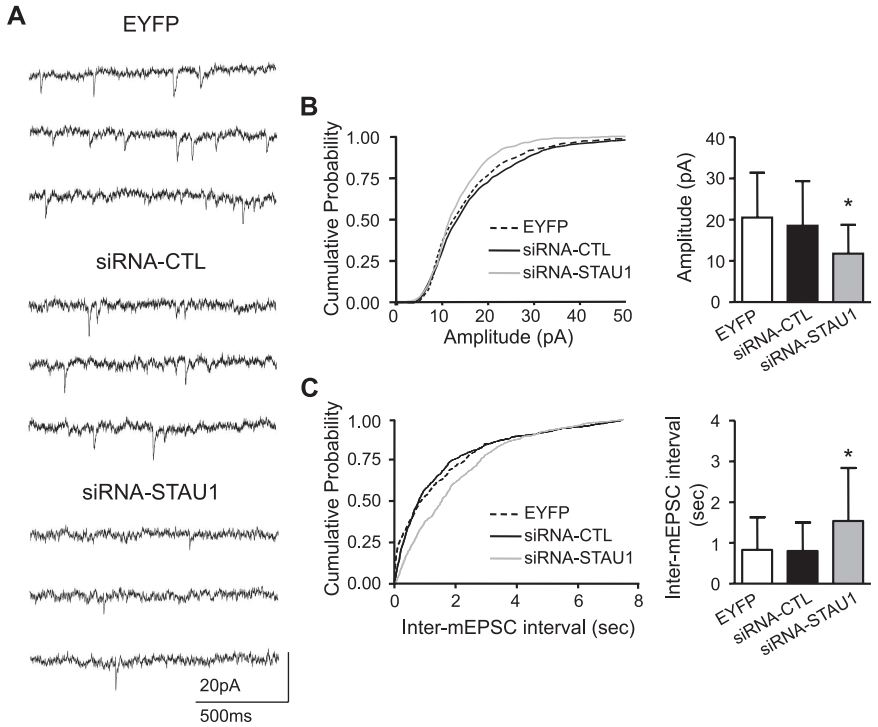

FIG. 6. Stau1 siRNA transfection reduces frequency and amplitude of mEPSCs. (A) Representative traces from pyramidal neurons transfected with plasmid coding for EYFP (top) or cotransfected with siRNA-CTL (middle) or siRNA-STAU1 (bottom). (B and C) Summary plots of cumulative distribution and summary bar graph of median of mEPSC amplitude (pA) (B) and inter-mEPSC intervals (s) (C) for the corresponding groups ($n = 7$ to 9 cells in each group), showing decrease in amplitude and frequency of mEPSCs in neurons transfected with siRNA-STAU1. Error bars represent standard deviations. *, $P < 0.001$.

reduction in regular spines (43.54% ± 6.35% compared to EYFP alone [EYFP]; 48.13% ± 7.02% compared to siRNA-CTL plus EYFP [siRNA-CTL]; $P < 0.05$) (Fig. 7D).

As an additional control, we repeated this experiment using a second interfering RNA (sh1) that targets a different Stau1 sequence. In addition, to confirm that the observed phenotype is the result of Stau1 down-regulation and not off-target effects, we expressed a Stau1 isoform that is not recognized by the shRNA (Stau1^{55}Δsh1) and determined whether this could rescue the phenotype. Spine density was unchanged in cells transfected with shRNA-CTL (0.26 ± 0.02 spines/μm), shRNA-STAU1/sh1 (0.31 ± 0.03 spines/μm), or shRNA-STAU1/sh1 plus Stau1^{55}Δsh1 (0.29 ± 0.02 spines/μm; $P > 0.05$) (Fig. 8B). However, spine length was significantly increased in cells transfected with shRNA-STAU1/sh1 relative to cells transfected with shRNA-CTL (113.45% ± 2.48%) or to cells cotransfected with shRNA-STAU1/sh1 plus Stau1^{55}Δsh1 (117.22% ± 2.56%) ($P < 0.05$; $n = 487$, 592, and 605 protrusions in shRNA-CTL, shRNA-STAU1/sh1, and shRNA-STAU1/sh1 plus Stau1^{55}Δsh1 groups, respectively; $n = 4$ to 6 separate experiments) (Fig. 8C). There was no significant difference between cells transfected with shRNA-CTL (1.21 ± 0.03 μm) and cells transfected with shRNA-STAU1/sh1 plus Stau1^{55}Δsh1 (1.18 ± 0.04 μm), indicating that expression of Stau1^{55}Δsh1 could rescue the effects of the shRNA-STAU1/sh1.

As shown in Fig. 8D, in cells transfected with shRNA-STAU1/sh1 there was a significant increase in the proportion of elongated spines to 131.68% ± 5.50% relative to cells transfected with shRNA-CTL. Cotransfection of Stau1^{55}Δsh1 and shRNA-STAU1/sh1 rescued the phenotype; the percentage of elongated spines in shRNA-STAU1/sh1-transfected cells was 147.02% ± 6.14% relative to cells cotransfected with Stau1^{55}Δsh1 and shRNA-STAU1/sh1 ($P < 0.05$) (Fig. 8D). Similarly for regular spines, in cells transfected with shRNA-STAU1/sh1 there was a significant decrease in their proportion to 65.40% ± 4.99% relative to cells transfected with shRNA-CTL. Again, cotransfection of Stau1^{55}Δsh1 and shRNA-STAU1/sh1 rescued the phenotype, and the percentage of regular spines in shRNA-STAU1/sh1-transfected cells was 61.88% ± 4.73% relative to cells cotransfected with Stau1^{55}Δsh1 and shRNA-STAU1/sh1 ($P < 0.05$) (Fig. 8D). There was no significant difference in the proportion of filopodia between the three conditions (shRNA-CTL, 10.56% ± 1.51%; shRNA-STAU1/sh1, 10.66% ± 1.34%; shRNA-STAU1/sh1 plus Stau1^{55}Δsh1, 9.02% ± 1.13%; $P > 0.05$) (Fig. 8D). Thus, transfection with shRNA-STAU1/sh1 resulted generally in similar effects as did transfection with siRNA-STAU1, except for the unchanged proportion of filopodia. It is possible that the sh1 interfering RNA endogenously produced from a plasmid following transfection is less effective in down-regulating Stau1 expression than the siRNA. It may also explain the reduced phenotype for spine length observed with Stau1 shRNA compared to Stau1 siRNA. Overall, this series of results indicate that the increase in spine length after transfection of Stau1 siRNA was due to a shift in spine shape from regular to elongated and filopodial types of spines. Thus, Stau1 down-regulation results in impairment of mature dendritic spine morphology.

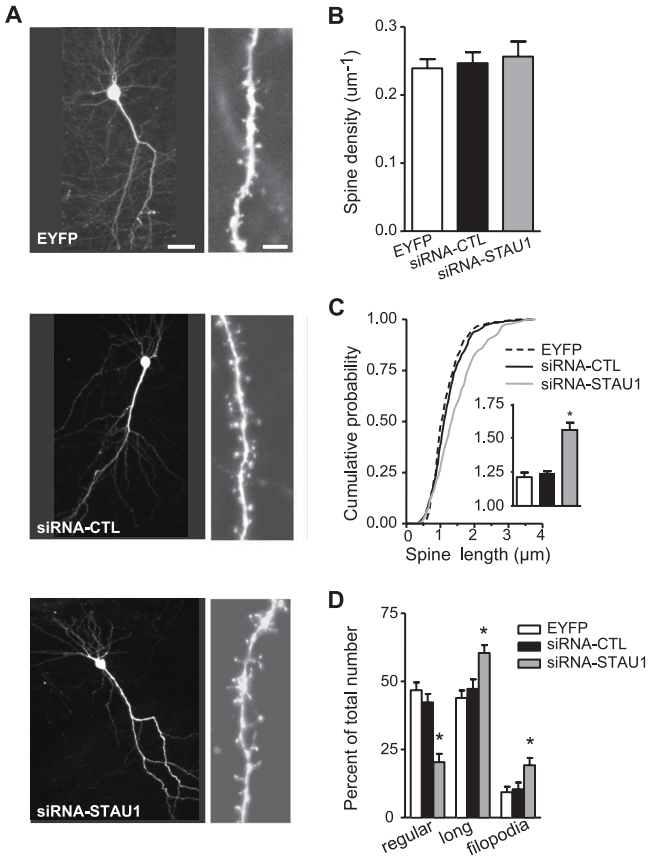

FIG. 7. Stau1 siRNA transfection affects dendritic spine morphology. (A) Confocal images of representative CA1 pyramidal cells (left) and apical dendrites (right) after transfection with plasmid coding for EYFP (top) or cotransfection with siRNA-CTL (middle) or siRNA-STAU1 (bottom). (B) Summary bar graph of spine density (per micrometer) of dendrite, showing unchanged density in all conditions. (C) Cumulative plots of the distribution of spine length for each group, with summary bar graph of spine length in the inset, showing increased spine length after transfection of siRNA-STAU1. (D) Summary bar graph of number of regular, elongated, or filopodium types of spines in cells of each group, showing decrease in regular and increases in elongated and filopodium types of spines after siRNA-STAU1 transfection. *, $P < 0.05$ (C and D).

DISCUSSION

Our principal findings are that Stau1 siRNA transfection results in selective down-regulation of Stau1 in hippocampal slice cultures, blocks specifically L-LTP without affecting E-LTP or LTD at pyramidal cell synapses, reduces spontaneous miniature synaptic activity, and alters morphology of mature dendritic spines of pyramidal cells. Our findings provide evidence for a key role for Stau1 in long-term plasticity and maintenance of mature synaptic connections in hippocampal neurons.

Expression of shRNAs and siRNAs can potentially trigger severe morphological and functional perturbations in neurons via off-target actions (1, 24, 49). Therefore, we performed several control experiments to validate our experimental approach of transfection in slice cultures. First, we confirmed with NeuN staining the absence of general morphological changes in hippocampal organization in slice cultures. Also, using confocal microscopy and imaging of individual EYFP-labeled cells, we found that dendritic arborizations of pyramidal neurons were unaffected by RNA interference transfection (1). Moreover, spine density was similar in all conditions and spine loss did not occur (1). Most importantly, we were able to rescue the phenotype of spine length and shape changes associated with Stau1 down-regulation by coexpression of a Stau1 isoform (Stau1$^{55}\Delta$sh1) not targeted by the Stau1 shRNA. Finally, input resistance and membrane capacitance, passive membrane properties that are affected by off-target actions (1), were unchanged in neurons transfected with siRNA. Hence, these results strongly indicate that down-regulation of the targeted protein Stau1, and not off-target actions, is responsible for the changes observed in this study.

Role of Stau1 in long-term synaptic plasticity. The late form of LTP is dependent on transcriptional and translational mechanisms (16, 41). Inhibition of de novo transcription impairs this L-LTP, without affecting the early form of LTP that requires posttranslational modification of preexisting proteins. Some of the transcripts generated during induction of L-LTP require local translation since focal dendritic application of protein synthesis inhibitors in slices inhibits L-LTP (5). Moreover, Ostroff et al. (43) have demonstrated the presence of polyribosome in dendritic spines, suggesting that local translation of new proteins may be enhanced at activated synaptic sites after LTP induction. Consistent with the established role of Stau1 in RNA transport (25, 29, 55), the impairment of L-LTP observed after Stau1 down-regulation is likely due to impaired transport of newly synthesized mRNAs. While we cannot rule out the possibility that other deficits in synaptic function seen after Stau1 down-regulation (changes in miniature synaptic activity and spine morphology) could also contribute to deficits in L-LTP, we think that this is unlikely for a number of reasons. First, basal evoked synaptic transmission, assessed by input-output curves and paired-pulse facilitation of fEPSPs, was unchanged after Stau1 siRNA transfection. Second, E-LTP and mGluR1/5-dependent LTD were not affected, suggesting that synapses and spines are intact and still capable of undergoing bidirectional plasticity. Third, the use of chemical LTP (32) obviates the possibility that a lack of sufficient synaptic drive during the induction protocol could explain the lack of L-LTP. Thus, we believe that the most parsimonious explanation is that impairment in L-LTP is due to the lack of transport and/or local translation of newly synthesized mRNAs.

There are additional correlative studies suggesting a role for RNA transport in late forms of synaptic plasticity and memory. In *Drosophila*, removal of Staufen reduces memory formation (11), although the mechanism of synaptic plasticity involved in this memory has not been established. Interestingly, Miller et al. (40) showed that removal of the native 3′ untranslated region of αCaMKII mRNA in mutant mice prevented dendritic localization of αCaMKII mRNA and decreased levels of αCaMKII in dendrites, as well as reducing L-LTP. Since Stau1 has been previously implicated in the transport of αCaMKII mRNA (25), our results would be consistent with a requirement for translation of αCaMKII for L-LTP. However, since in this particular study (40) levels of αCaMKII in dendrites were severely decreased before stimulation, it is unclear whether the deficit in long-term memory was due to the acute lack of translation of αCaMKII after tetanization.

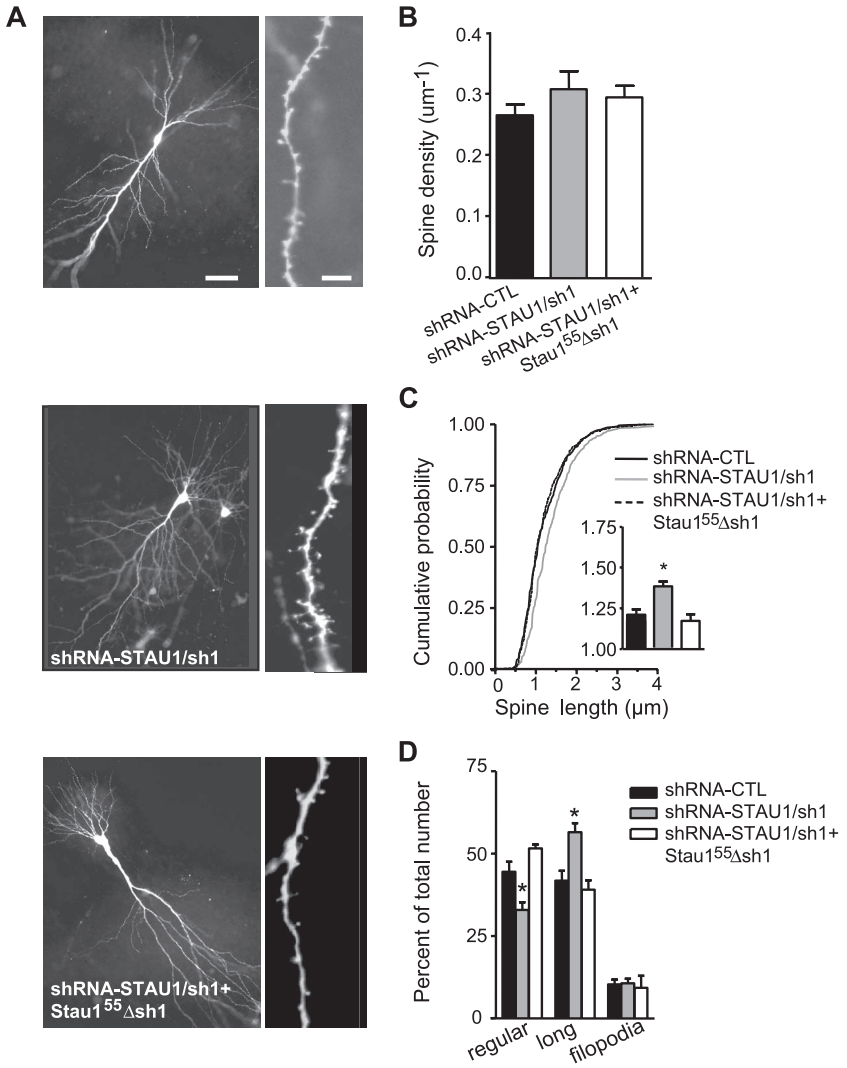

FIG. 8. Dendritic spine morphology changes induced by Stau1 down-regulation using Stau1 shRNA and rescue by coexpression of Stau1^{55}Δsh1. (A) Confocal images of representative CA1 pyramidal cells (left) and apical dendrites (right) after cotransfection of plasmid coding for EYFP and shRNA-CTL (top), shRNA-STAU1/sh1 (middle), or shRNA-STAU1/sh1 plus Stau1^{55}Δsh1 (bottom). (B) Summary bar graph of spine density (per micrometer) of dendrite, showing unchanged density in all conditions. (C) Cumulative plots of the distribution of spine length for each group, with summary bar graph of spine length in the inset, showing increased spine length after transfection of shRNA-STAU1/sh1 and rescue by shRNA-STAU1/sh1 plus Stau1^{55}Δsh1 transfection. (D) Summary bar graph of number of regular, elongated, or filopodium types of spines in cells of each group, showing decrease in regular and increases in elongated types of spines after shRNA-STAU1/sh1 transfection and rescue by shRNA-STAU1/sh1 plus Stau1^{55}Δsh1 transfection. *, $P < 0.05$ (C and D).

Role of Stau1 in spine morphogenesis and spontaneous miniature synaptic activity. Dendritic spines are thought to act as functional units, providing microcompartments for segregating postsynaptic chemical responses, such as calcium elevation (46, 63), and for integrating synaptic signals. The significant increase in the percentage of elongated spines and filopodium-like protrusions after Stau1 down-regulation suggests a close relationship between Stau1 and dendritic spine morphology. The size of the spine head is proportional to the PSDs, the number of postsynaptic α-amino-3-hydroxy-5-methylisoxazole-4-propionic acid (AMPA) receptors (42, 48, 59), suggesting that growth of the spine head correlates with strengthening of the synapse. Moreover, elongated spines and filopodium-like protrusions have been shown to be postsynaptic components of silent synapses (38). Therefore, an increase in elongated spines and filopodium-like protrusions after Stau1 down-regulation could possibly reflect a down-regulation of synaptic function. This is consistent with the decrease in mEPSC frequency and amplitude seen in this study. Interestingly, in several studies of fragile X syndrome (9, 19, 64), the marked increase in the proportion of elongated spines and filopodium-like protrusions is similar to the effect observed with Stau1 down-regulation. Stau1 and FMRP (Fragile X mental retardation protein) may have similar functions in regulating RNA transport and/or translation.

Staufen isoforms and functional implications. Another important finding is that the alterations of spine morphology observed with Stau1 down-regulation have clear correlated functional consequences. We found a reduction in amplitude

and frequency of spontaneous miniature synaptic activity that is consistent with the observed reduction in the number of regular spines and hypothesized increase in number of silent synapses (38). Thus, Stau1 appears to be involved in the maintenance of mature spine morphology and excitatory synaptic activity. Interestingly, basal evoked synaptic transmission, assessed by fEPSP input-output curves, paired-pulse facilitation, E-LTP and mGluR1/5 LTD induction, was unchanged after siRNA transfection, suggesting that other parallel changes, likely involving inhibitory synaptic function, also take place after Stau1 down-regulation, which results in normal levels of excitability in hippocampal networks.

A recent study suggests that the other Staufen paralogue, Stau2, has an important role in the formation and maintenance of synapses and dendritic spines in cultured hippocampal neurons (18). After Stau2 down-regulation, a significant reduction in the number of dendritic spines and an increase in filopodium-like protrusions were noted. Also, the number of PSD-95-positive synapses and mEPSC amplitude were markedly reduced. The differences observed after Stau2 down-regulation and those reported here suggest that the two paralogues may have distinct, but related, functions. Notably, the observed reduction in spine density after Stau2 down-regulation indicates that this isoform is involved in synapse formation and spine morphogenesis (18), while we observe no decreases in the number of spines, suggesting that Stau1 is more involved in synaptic plasticity and associated spine morphology changes. Interestingly, no decrease was observed in mEPSC frequency after Stau2 down-regulation in cultured neurons. It is possible that the environment of cultured neurons may be less permissive for the formation of silent synapses than the environment in hippocampal slice cultures, and thus, the difference in model systems may explain the lack of change in mEPSC frequency. Alternatively, the decrease in mEPSC frequency observed after Stau1 down-regulation may be related to the deficit in L-LTP which was also present. Stau1 and Stau2 do not colocalize with each other in distal dendrites, suggesting that these proteins are located in distinct RNA granules (12). Stau1 is known to participate in translational control, consistent with our data for distinct roles of Stau1 and Stau2 in the formation of synapses and spines during development (18). This suggests that different transport mechanisms are used for different pools of mRNAs, an idea which is also supported by the multiple classes of RNA transport particles and granules identified in neurons (14, 50).

Our findings with Stau1 shed some light on the importance of mRNA transport to dendrites for regulating synaptic function and long-term plasticity. It will be interesting to examine how Staufen paralogues are associated with RNA granules and whether different RNA granules containing Stau1 and Stau2 transport different sets of mRNA. These are important questions to understand further the role of RNA-binding proteins and mRNA trafficking in synaptic plasticity and associated functional connectivity changes underlying hippocampus-dependent learning and memory.

ACKNOWLEDGMENTS

We thank Julie Pepin for excellent technical assistance.

This research was supported by the Canadian Institutes of Health Research (Synaptic Transmission and Plasticity Group) and the Canada Research Chair Program (J.-C.L.; Canada Research Chair in Cellular and Molecular Neurophysiology). W.S. is a William Dawson scholar and FRSQ Chercheur National. G.L. and L.T. were supported by the Savoy Foundation. M.M.-L. was supported by a studentship from the Natural Sciences and Engineering Research Council of Canada.

REFERENCES

1. **Alvarez, V. A., D. A. Ridenour, and B. L. Sabatini.** 2006. Retraction of synapses and dendritic spines induced by off-target effects of RNA interference. J. Neurosci. **26:**7820–7825.
2. **Antar, L. N., R. Afroz, J. B. Dictenberg, R. C. Carroll, and G. J. Bassell.** 2004. Metabotropic glutamate receptor activation regulates fragile X mental retardation protein and FMR1 mRNA localization differentially in dendrites and at synapses. J. Neurosci. **24:**2648–2655.
3. **Banker, G., and K. Goslin.** 1988. Developments in neuronal cell culture. Nature **336:**185–186.
4. **Bourdeau, M. L., F. Morin, C. E. Laurent, M. Azzi, and J. C. Lacaille.** 2007. Kv4.3-mediated A-type K+ currents underlie rhythmic activity in hippocampal interneurons. J. Neurosci. **27:**1942–1953.
5. **Bradshaw, K. D., N. J. Emptage, and T. V. Bliss.** 2003. A role for dendritic protein synthesis in hippocampal late LTP. Eur. J. Neurosci. **18:**3150–3152.
6. **Broadus, J., S. Fuerstenberg, and C. Q. Doe.** 1998. Staufen-dependent localization of prospero mRNA contributes to neuroblast daughter-cell fate. Nature **391:**792–795.
7. **Buchner, G., M. T. Bassi, G. Andolfi, A. Ballabio, and B. Franco.** 1999. Identification of a novel homolog of the Drosophila staufen protein in the chromosome 8q13-q21.1 region. Genomics **62:**113–118.
8. **Chavez-Noriega, L. E., and C. F. Stevens.** 1992. Modulation of synaptic efficacy in field CA1 of the rat hippocampus by forskolin. Brain Res. **574:**85–92.
9. **Comery, T. A., J. B. Harris, P. J. Willems, B. A. Oostra, S. A. Irwin, I. J. Weiler, and W. T. Greenough.** 1997. Abnormal dendritic spines in fragile X knockout mice: maturation and pruning deficits. Proc. Natl. Acad. Sci. USA **94:**5401–5404.
10. **DesGroseillers, L., and N. Lemieux.** 1996. Localization of a human double-stranded RNA-binding protein gene (STAU) to band 20q13.1 by fluorescence in situ hybridization. Genomics **36:**527–529.
11. **Dubnau, J., A. S. Chiang, L. Grady, J. Barditch, S. Gossweiler, J. McNeil, P. Smith, F. Buldoc, R. Scott, U. Certa, C. Broger, and T. Tully.** 2003. The staufen/pumilio pathway is involved in Drosophila long-term memory. Curr. Biol. **13:**286–296.
12. **Duchaine, T. F., I. Hemraj, L. Furic, A. Deitinghoff, M. A. Kiebler, and L. DesGroseillers.** 2002. Staufen2 isoforms localize to the somatodendritic domain of neurons and interact with different organelles. J. Cell Sci. **115:**3285–3295.
13. **Dugre-Brisson, S., G. Elvira, K. Boulay, L. Chatel-Chaix, A. J. Mouland, and L. DesGroseillers.** 2005. Interaction of Staufen1 with the 5′ end of mRNA facilitates translation of these RNAs. Nucleic Acids Res. **33:**4797–4812.
14. **Elvira, G., B. Massie, and L. DesGroseillers.** 2006. The zinc-finger protein ZFR is critical for Staufen 2 isoform specific nucleocytoplasmic shuttling in neurons. J. Neurochem. **96:**105–117.
15. **Fitzjohn, S. M., A. E. Kingston, D. Lodge, and G. L. Collingridge.** 1999. DHPG-induced LTD in area CA1 of juvenile rat hippocampus; characterisation and sensitivity to novel mGlu receptor antagonists. Neuropharmacology **38:**1577–1583.
16. **Frey, U., M. Krug, K. G. Reymann, and H. Matthies.** 1988. Anisomycin, an inhibitor of protein synthesis, blocks late phases of LTP phenomena in the hippocampal CA1 region in vitro. Brain Res. **452:**57–65.
17. **Gelinas, J. N., and P. V. Nguyen.** 2005. Beta-adrenergic receptor activation facilitates induction of a protein synthesis-dependent late phase of long-term potentiation. J. Neurosci. **25:**3294–3303.
18. **Goetze, B., F. Tuebing, Y. Xie, M. M. Dorostkar, S. Thomas, U. Pehl, S. Boehm, P. Macchi, and M. A. Kiebler.** 2006. The brain-specific double-stranded RNA-binding protein Staufen2 is required for dendritic spine morphogenesis. J. Cell Biol. **172:**221–231.
19. **Greenough, W. T., A. Y. Klintsova, S. A. Irwin, R. Galvez, K. E. Bates, and I. J. Weiler.** 2001. Synaptic regulation of protein synthesis and the fragile X protein. Proc. Natl. Acad. Sci. USA **98:**7101–7106.
20. **Harris, K. M., and J. K. Stevens.** 1989. Dendritic spines of CA 1 pyramidal cells in the rat hippocampus: serial electron microscopy with reference to their biophysical characteristics. J. Neurosci. **9:**2982–2997.
21. **Huang, Y. Y., X. C. Li, and E. R. Kandel.** 1994. cAMP contributes to mossy fiber LTP by initiating both a covalently mediated early phase and macromolecular synthesis-dependent late phase. Cell **79:**69–79.
22. **Huber, K. M., M. S. Kayser, and M. F. Bear.** 2000. Role for rapid dendritic protein synthesis in hippocampal mGluR-dependent long-term depression. Science **288:**1254–1257.
23. **Huber, K. M., N. B. Sawtell, and M. F. Bear.** 1998. Effects of the metabotropic glutamate receptor antagonist MCPG on phosphoinositide turnover and synaptic plasticity in visual cortex. J. Neurosci. **18:**1–9.

24. **Judge, A. D., V. Sood, J. R. Shaw, D. Fang, K. McClintock, and I. MacLachlan.** 2005. Sequence-dependent stimulation of the mammalian innate immune response by synthetic siRNA. Nat. Biotechnol. **23:**457–462.
25. **Kanai, Y., N. Dohmae, and N. Hirokawa.** 2004. Kinesin transports RNA: isolation and characterization of an RNA-transporting granule. Neuron **43:** 513–525.
26. **Kelleher, R. J., III, A. Govindarajan, H. Y. Jung, H. Kang, and S. Tonegawa.** 2004. Translational control by MAPK signaling in long-term synaptic plasticity and memory. Cell **116:**467–479.
27. **Kiebler, M. A., and L. DesGroseillers.** 2000. Molecular insights into mRNA transport and local translation in the mammalian nervous system. Neuron **25:**19–28.
28. **Kiebler, M. A., I. Hemraj, P. Verkade, M. Kohrmann, P. Fortes, R. M. Marion, J. Ortin, and C. G. Dotti.** 1999. The mammalian staufen protein localizes to the somatodendritic domain of cultured hippocampal neurons: implications for its involvement in mRNA transport. J. Neurosci. **19:**288–297.
29. **Kim, K. C., and H. K. Kim.** 2006. Role of Staufen in dendritic mRNA transport and its modulation. Neurosci. Lett. **397:**48–52.
30. **Kim, Y. K., L. Furic, L. Desgroseillers, and L. E. Maquat.** 2005. Mammalian Staufen1 recruits Upf1 to specific mRNA 3′UTRs so as to elicit mRNA decay. Cell **120:**195–208.
31. **Kohrmann, M., M. Luo, C. Kaether, L. DesGroseillers, C. G. Dotti, and M. A. Kiebler.** 1999. Microtubule-dependent recruitment of Staufen-green fluorescent protein into large RNA-containing granules and subsequent dendritic transport in living hippocampal neurons. Mol. Biol. Cell **10:**2945–2953.
32. **Kopec, C. D., B. Li, W. Wei, J. Boehm, and R. Malinow.** 2006. Glutamate receptor exocytosis and spine enlargement during chemically induced long-term potentiation. J. Neurosci. **26:**2000–2009.
33. **Krichevsky, A. M., and K. S. Kosik.** 2001. Neuronal RNA granules: a link between RNA localization and stimulation-dependent translation. Neuron **32:**683–696.
34. **Luo, M., T. F. Duchaine, and L. DesGroseillers.** 2002. Molecular mapping of the determinants involved in human Staufen-ribosome association. Biochem. J. **365:**817–824.
35. **Manabe, T., P. Renner, and R. A. Nicoll.** 1992. Postsynaptic contribution to long-term potentiation revealed by the analysis of miniature synaptic currents. Nature **355:**50–55.
36. **Marion, R. M., P. Fortes, A. Beloso, C. Dotti, and J. Ortin.** 1999. A human sequence homologue of Staufen is an RNA-binding protein that is associated with polysomes and localizes to the rough endoplasmic reticulum. Mol. Cell. Biol. **19:**2212–2219.
37. **Matsuzaki, F., T. Ohshiro, H. Ikeshima-Kataoka, and H. Izumi.** 1998. miranda localizes staufen and prospero asymmetrically in mitotic neuroblasts and epithelial cells in early Drosophila embryogenesis. Development **125:** 4089–4098.
38. **Matsuzaki, M., G. C. Ellis-Davies, T. Nemoto, Y. Miyashita, M. Iino, and H. Kasai.** 2001. Dendritic spine geometry is critical for AMPA receptor expression in hippocampal CA1 pyramidal neurons. Nat. Neurosci. **4:**1086–1092.
39. **McKinney, R. A.** 2005. Physiological roles of spine motility: development, plasticity and disorders. Biochem. Soc. Trans. **33:**1299–1302.
40. **Miller, S., M. Yasuda, J. K. Coats, Y. Jones, M. E. Martone, and M. Mayford.** 2002. Disruption of dendritic translation of CaMKIIalpha impairs stabilization of synaptic plasticity and memory consolidation. Neuron **36:** 507–519.
41. **Nguyen, P. V., T. Abel, and E. R. Kandel.** 1994. Requirement of a critical period of transcription for induction of a late phase of LTP. Science **265:** 1104–1107.
42. **Nusser, Z., R. Lujan, G. Laube, J. D. Roberts, E. Molnar, and P. Somogyi.** 1998. Cell type and pathway dependence of synaptic AMPA receptor number and variability in the hippocampus. Neuron **21:**545–559.
43. **Ostroff, L. E., J. C. Fiala, B. Allwardt, and K. M. Harris.** 2002. Polyribosomes redistribute from dendritic shafts into spines with enlarged synapses during LTP in developing rat hippocampal slices. Neuron **35:**535–545.
44. **Otmakhov, N., L. Khibnik, N. Otmakhova, S. Carpenter, S. Riahi, B. Asrican, and J. Lisman.** 2004. Forskolin-induced LTP in the CA1 hippocampal region is NMDA receptor dependent. J. Neurophysiol. **91:**1955–1962.
45. **Pierce, J. P., K. van Leyen, and J. B. McCarthy.** 2000. Translocation machinery for synthesis of integral membrane and secretory proteins in dendritic spines. Nat. Neurosci. **3:**311–313.
46. **Sabatini, B. L., M. Maravall, and K. Svoboda.** 2001. Ca(2+) signaling in dendritic spines. Curr. Opin. Neurobiol. **11:**349–356.
47. **Scanziani, M., M. Capogna, B. H. Gahwiler, and S. M. Thompson.** 1992. Presynaptic inhibition of miniature excitatory synaptic currents by baclofen and adenosine in the hippocampus. Neuron **9:**919–927.
48. **Shi, S. H., Y. Hayashi, R. S. Petralia, S. H. Zaman, R. J. Wenthold, K. Svoboda, and R. Malinow.** 1999. Rapid spine delivery and redistribution of AMPA receptors after synaptic NMDA receptor activation. Science **284:** 1811–1816.
49. **Sledz, C. A., M. Holko, M. J. de Veer, R. H. Silverman, and B. R. Williams.** 2003. Activation of the interferon system by short-interfering RNAs. Nat. Cell Biol. **5:**834–839.
50. **Sossin, W. S., and L. DesGroseillers.** 2006. Intracellular trafficking of RNA in neurons. Traffic **7:**1581–1589.
51. **Steward, O., and E. M. Schuman.** 2001. Protein synthesis at synaptic sites on dendrites. Annu. Rev. Neurosci. **24:**299–325.
52. **St Johnston, D.** 1995. The intracellular localization of messenger RNAs. Cell **81:**161–170.
53. **Stoppini, L., P. A. Buchs, and D. Muller.** 1991. A simple method for organotypic cultures of nervous tissue. J. Neurosci. Methods **37:**173–182.
54. **Sutton, M. A., and E. M. Schuman.** 2006. Dendritic protein synthesis, synaptic plasticity, and memory. Cell **127:**49–58.
55. **Tang, S. J., D. Meulemans, L. Vazquez, N. Colaco, and E. Schuman.** 2001. A role for a rat homolog of staufen in the transport of RNA to neuronal dendrites. Neuron **32:**463–475.
56. **Tang, S. J., and E. M. Schuman.** 2002. Protein synthesis in the dendrite. Philos. Trans. R. Soc. Lond. B Biol. Sci. **357:**521–529.
57. **Thomas, M. G., L. J. Martinez Tosar, M. Loschi, J. M. Pasquini, J. Correale, S. Kindler, and G. L. Boccaccio.** 2005. Staufen recruitment into stress granules does not affect early mRNA transport in oligodendrocytes. Mol. Biol. Cell **16:**405–420.
58. **Tiedge, H., and J. Brosius.** 1996. Translational machinery in dendrites of hippocampal neurons in culture. J. Neurosci. **16:**7171–7181.
59. **Turrigiano, G. G.** 2000. AMPA receptors unbound: membrane cycling and synaptic plasticity. Neuron **26:**5–8.
60. **Volk, L. J., C. A. Daly, and K. M. Huber.** 2006. Differential roles for group 1 mGluR subtypes in induction and expression of chemically induced hippocampal long-term depression. J. Neurophysiol. **95:**2427–2438.
61. **Wickham, L., T. Duchaine, M. Luo, I. R. Nabi, and L. DesGroseillers.** 1999. Mammalian staufen is a double-stranded-RNA- and tubulin-binding protein which localizes to the rough endoplasmic reticulum. Mol. Cell. Biol. **19:** 2220–2230.
62. **Wong, S. T., J. Athos, X. A. Figueroa, V. V. Pineda, M. L. Schaefer, C. C. Chavkin, L. J. Muglia, and D. R. Storm.** 1999. Calcium-stimulated adenylyl cyclase activity is critical for hippocampus-dependent long-term memory and late phase LTP. Neuron **23:**787–798.
63. **Yuste, R., and W. Denk.** 1995. Dendritic spines as basic functional units of neuronal integration. Nature **375:**682–684.
64. **Zalfa, F., T. Achsel, and C. Bagni.** 2006. mRNPs, polysomes or granules: FMRP in neuronal protein synthesis. Curr. Opin. Neurobiol. **16:**265–269.